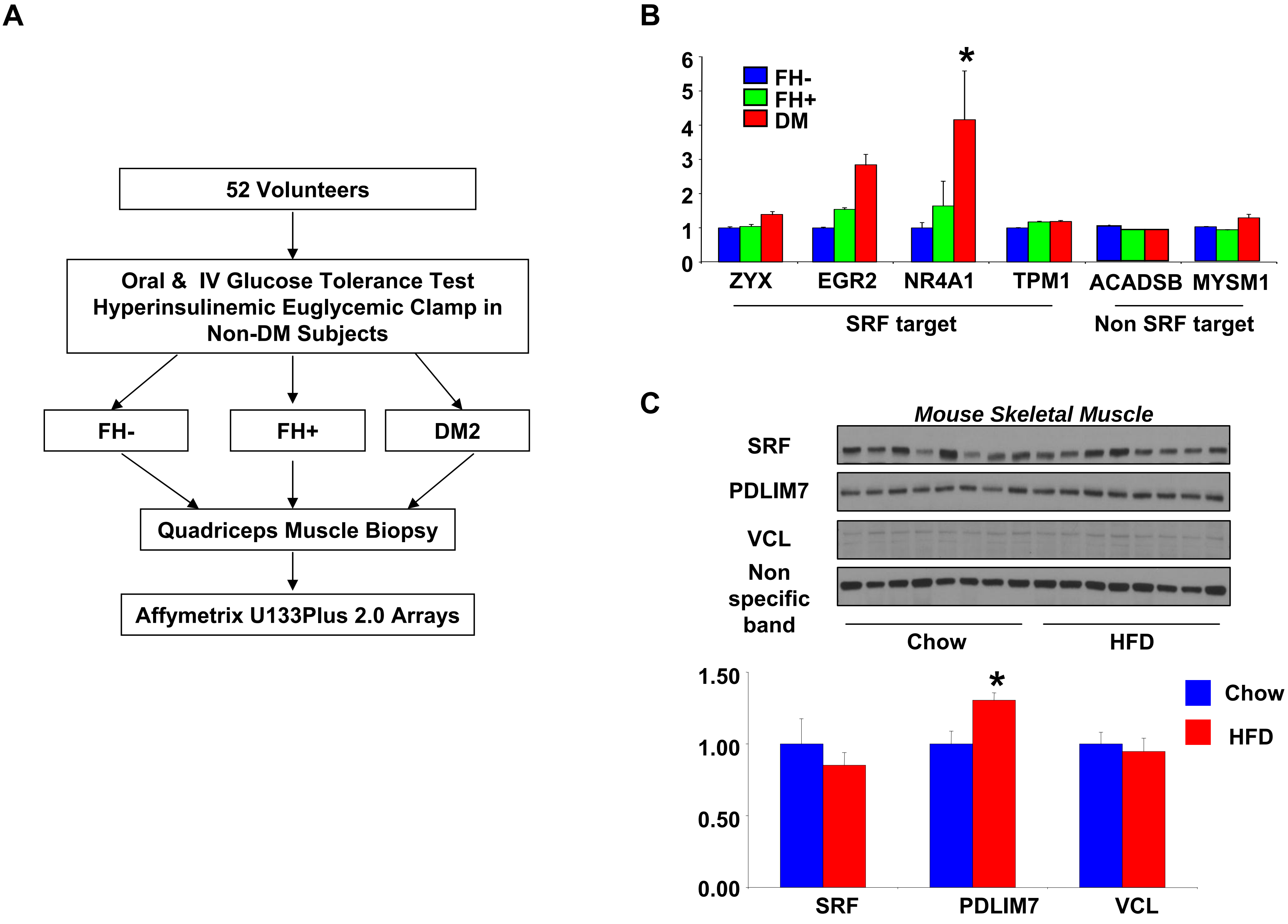

Supplemental Fig. 1. Jin et al

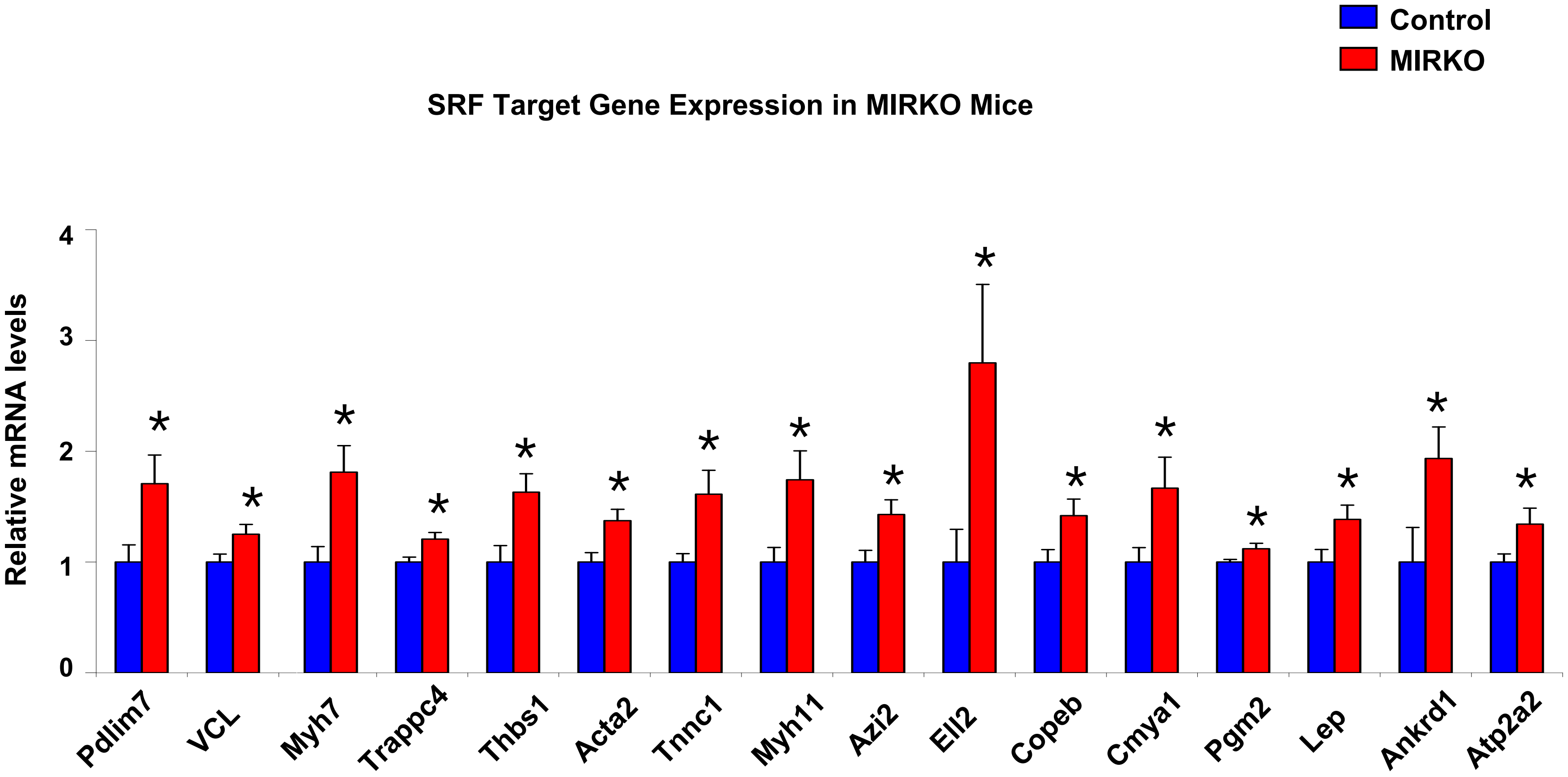

SRF Target Gene Expression in MIRKO Mice

Supplemental Fig. 2. Jin et al

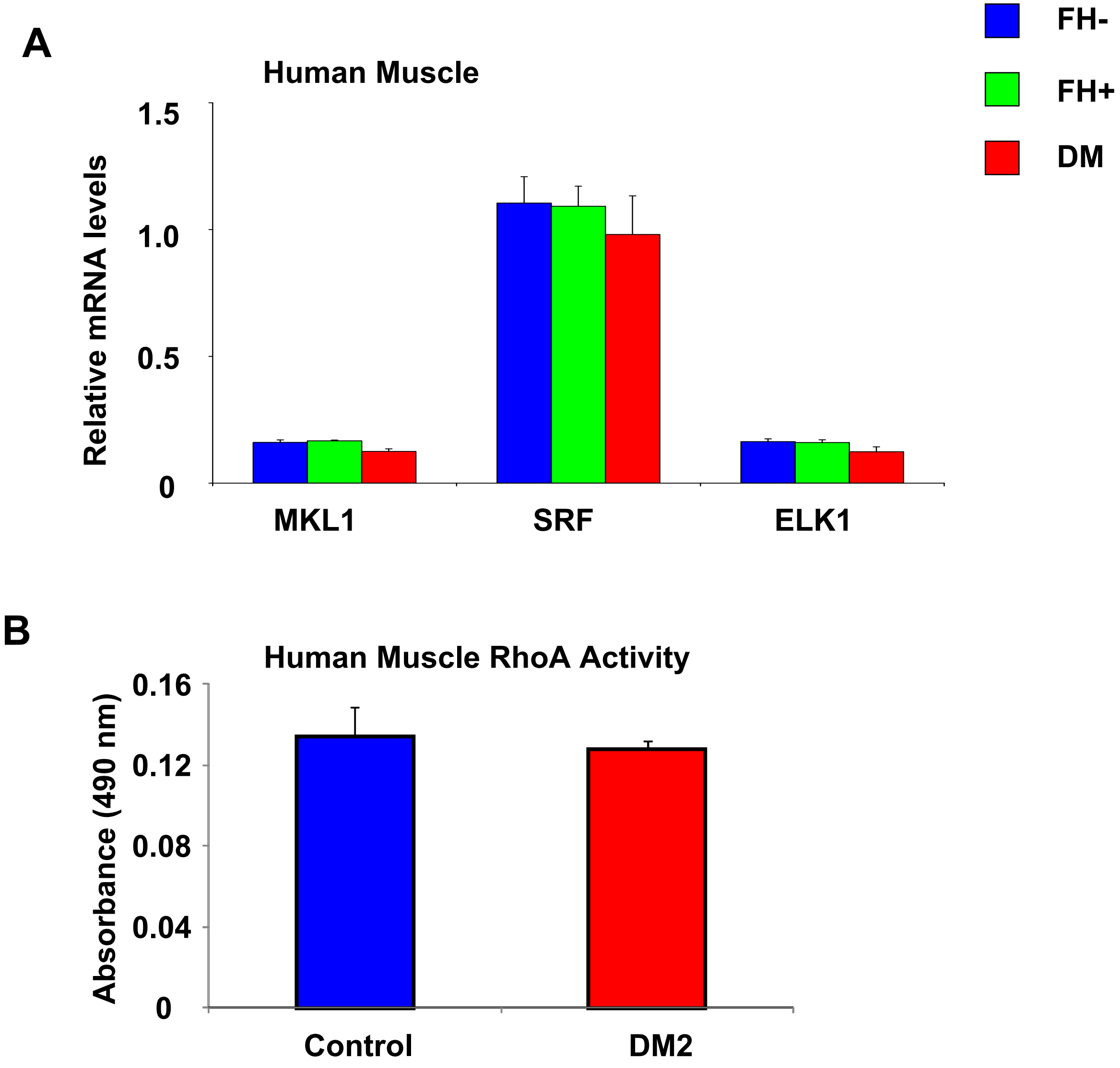

Supplemental Fig. 3. Jin et al

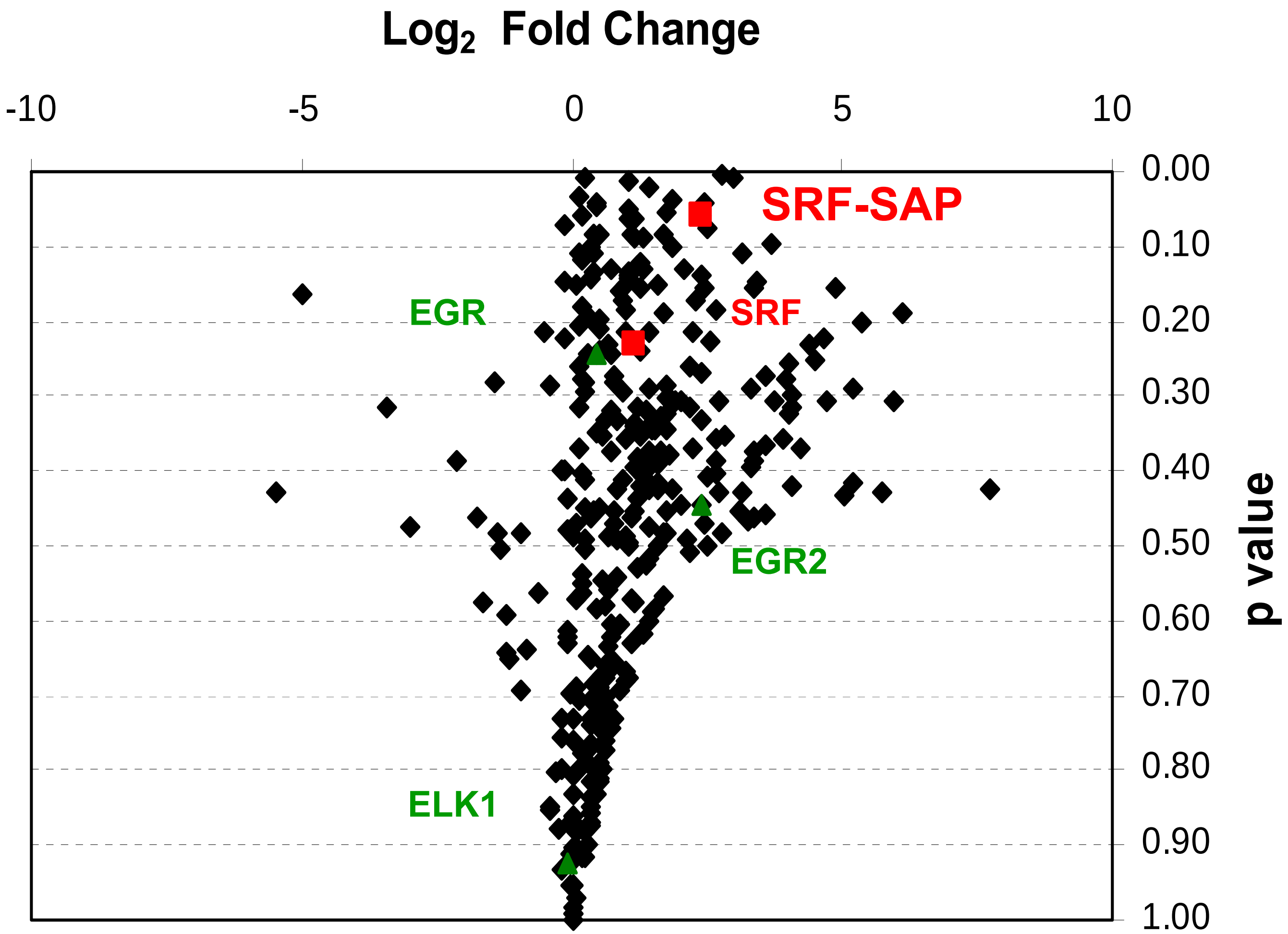

Supplemental Fig. 4. Jin et al

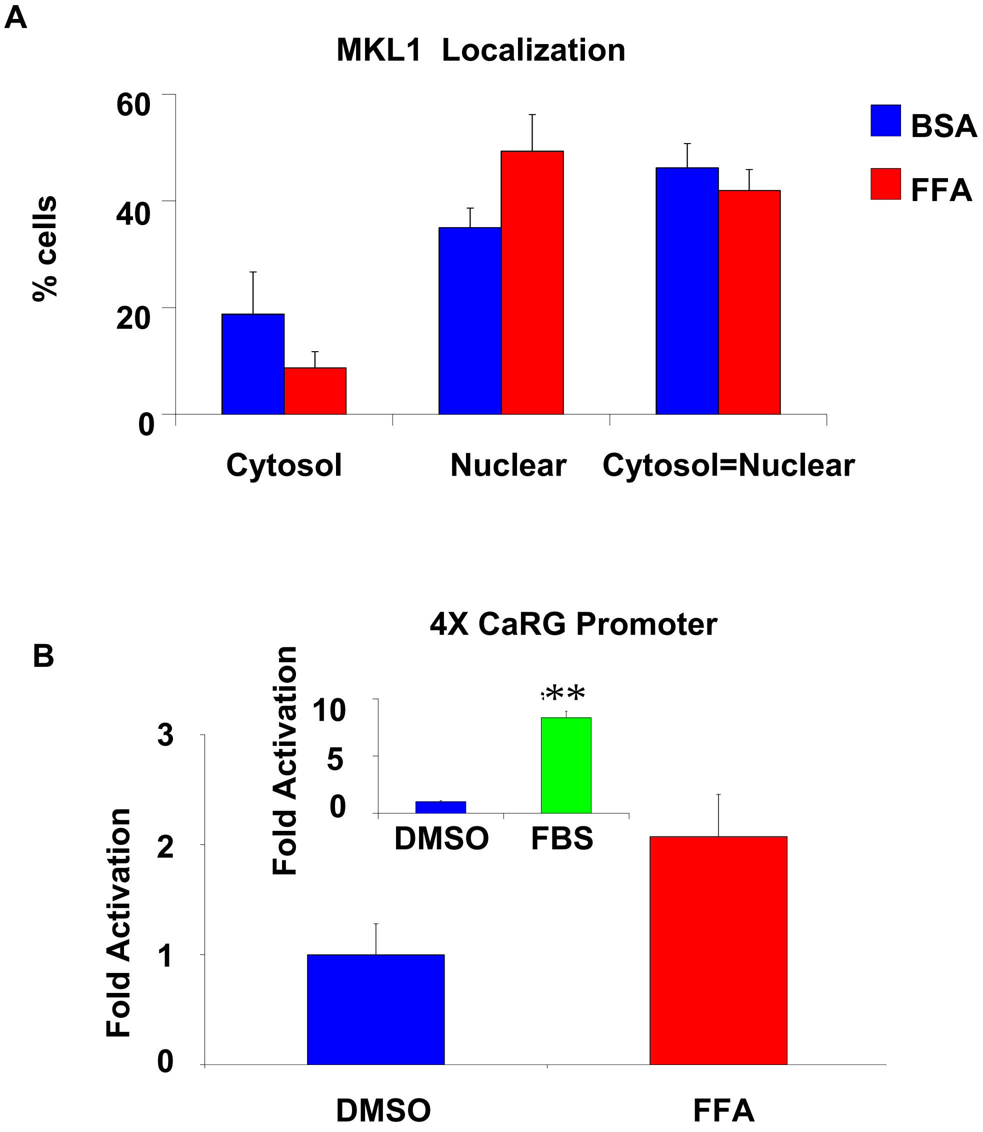

Supplemental Fig. 5. Jin et al

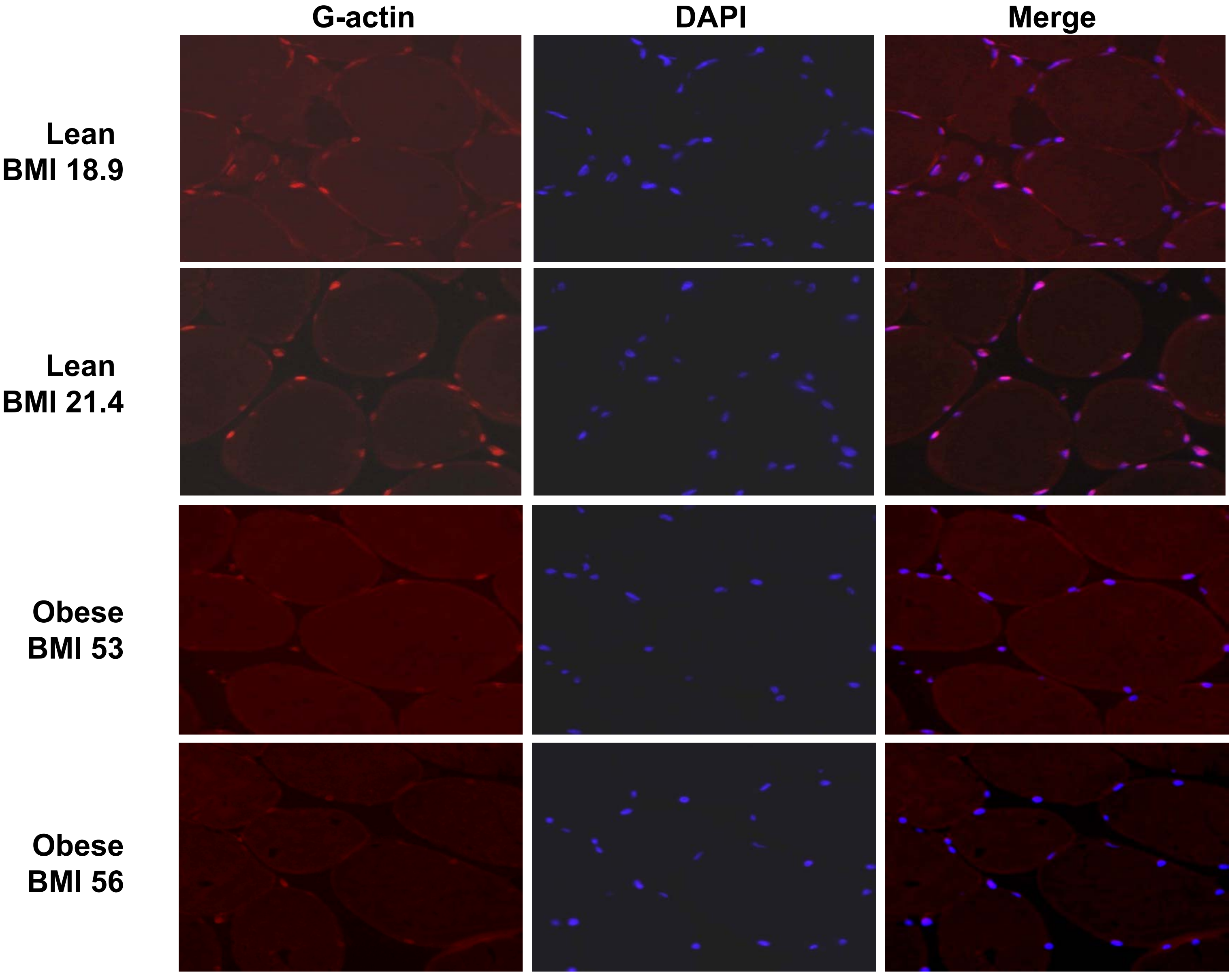

Supplemental Fig. 6. Jin et al

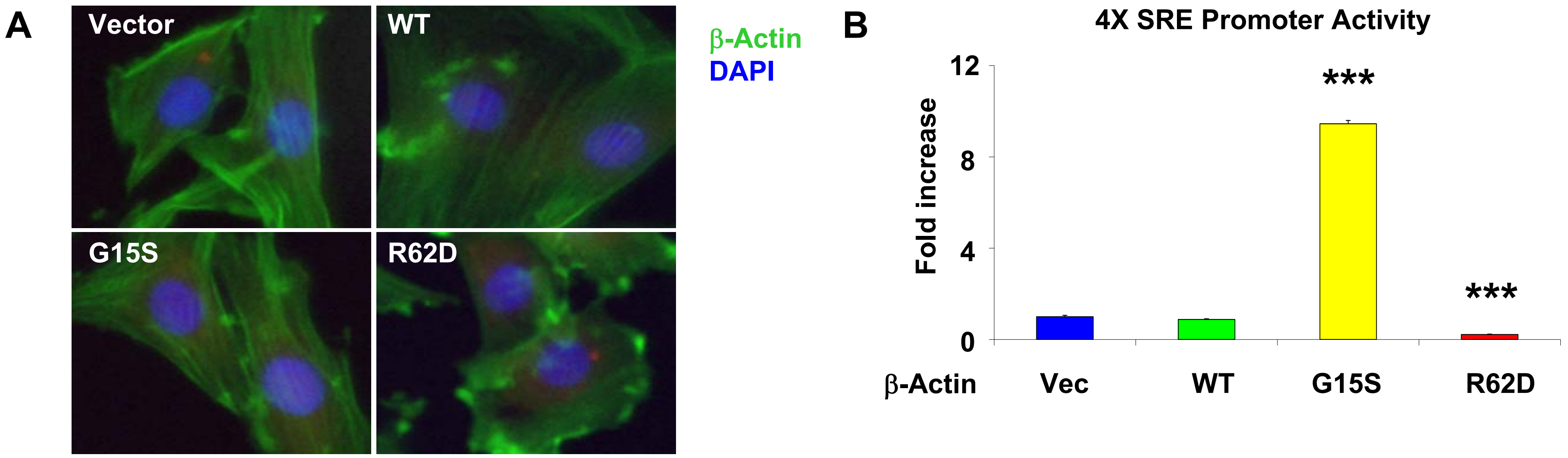

Supplemental Fig. 7. Jin et al

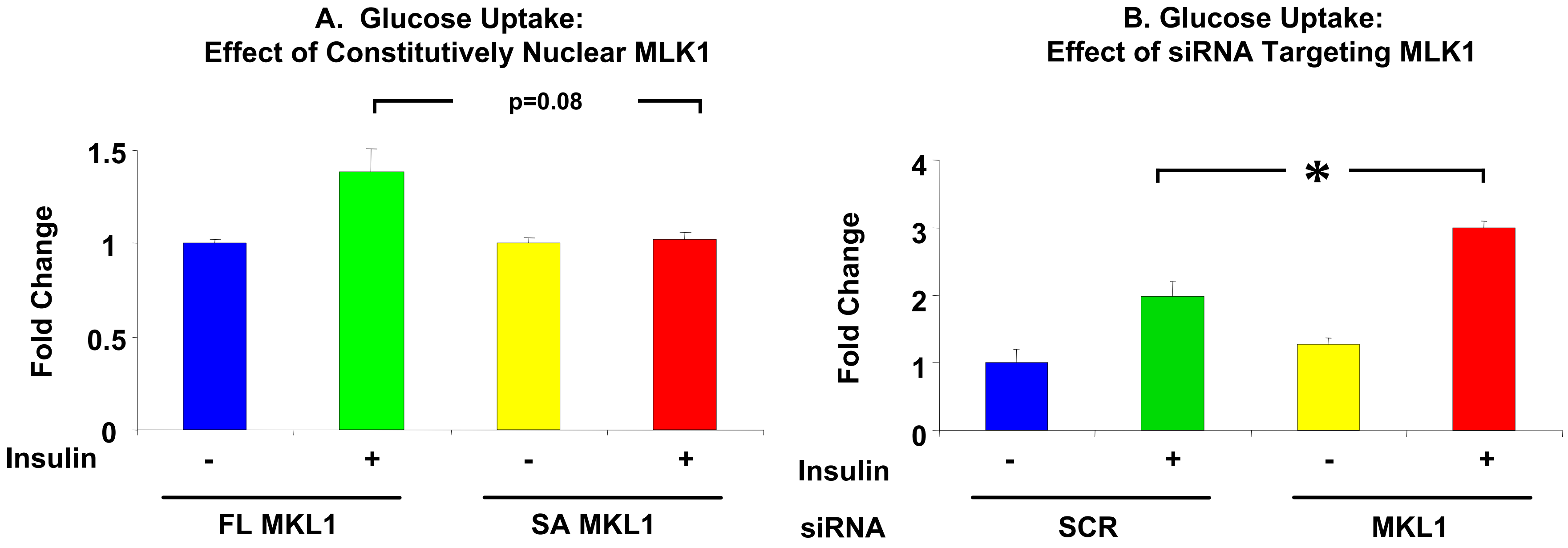
A. Glucose Uptake: Effect of Constitutively Nuclear MLK1

B. Glucose Uptake: Effect of siRNA Targeting MLK1

Supplemental Fig. 8. Jin et al

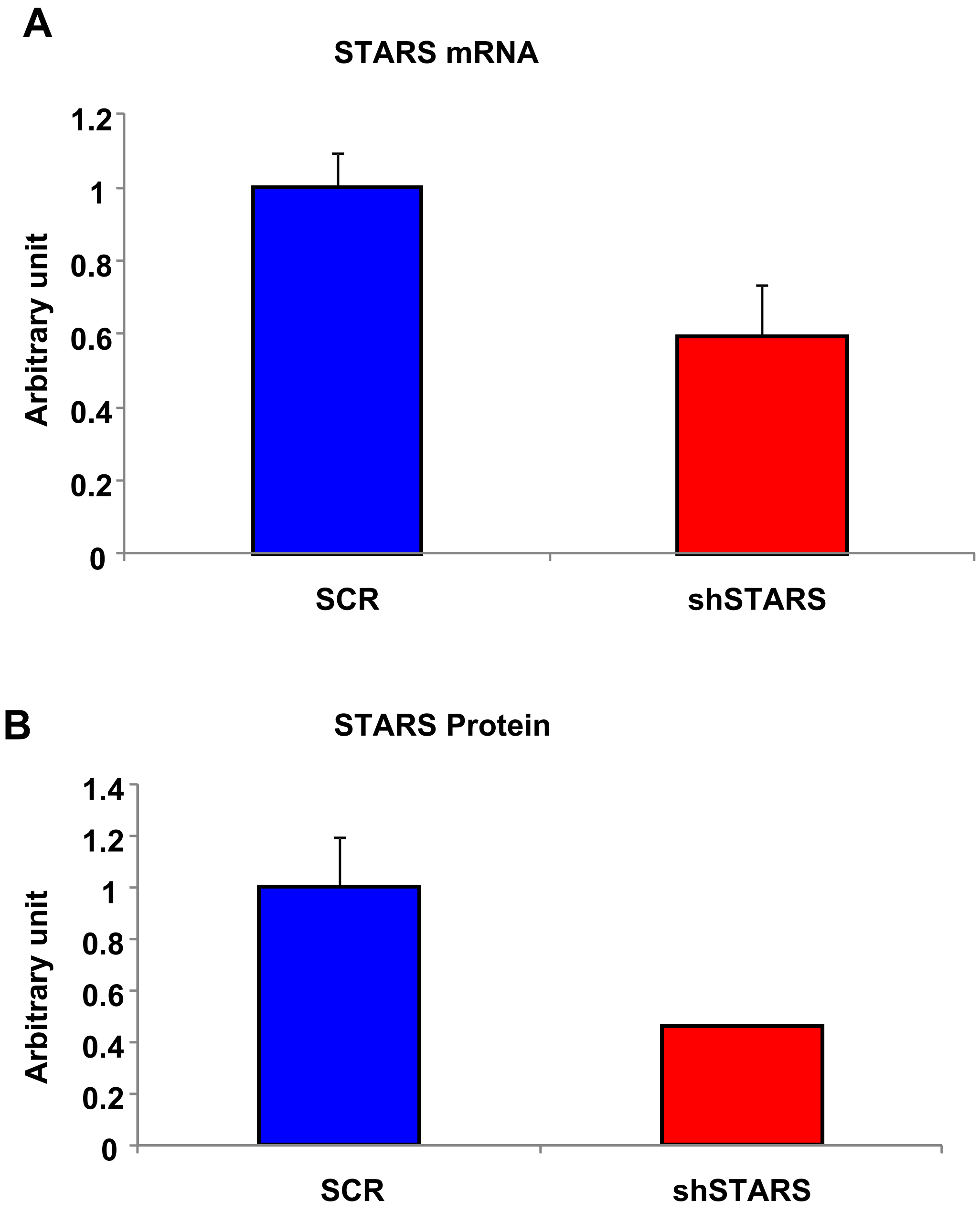

Supplemental Fig. 9. Jin et al.

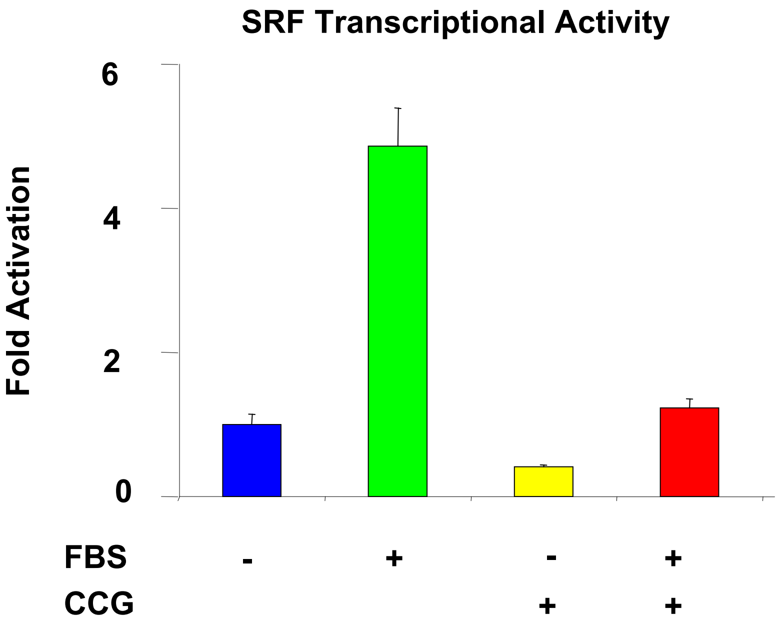

Supplemental Fig. 10. Jin et al.

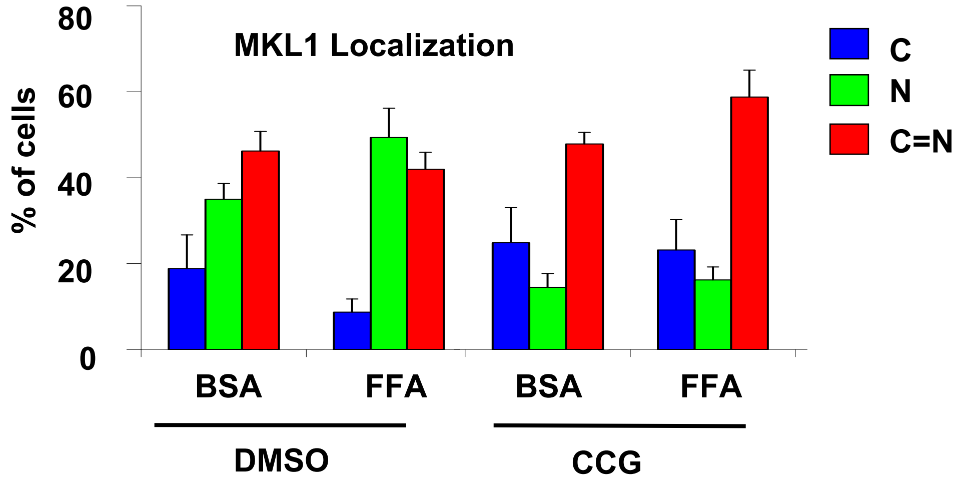

Supplemental Fig. 11. Jin et al

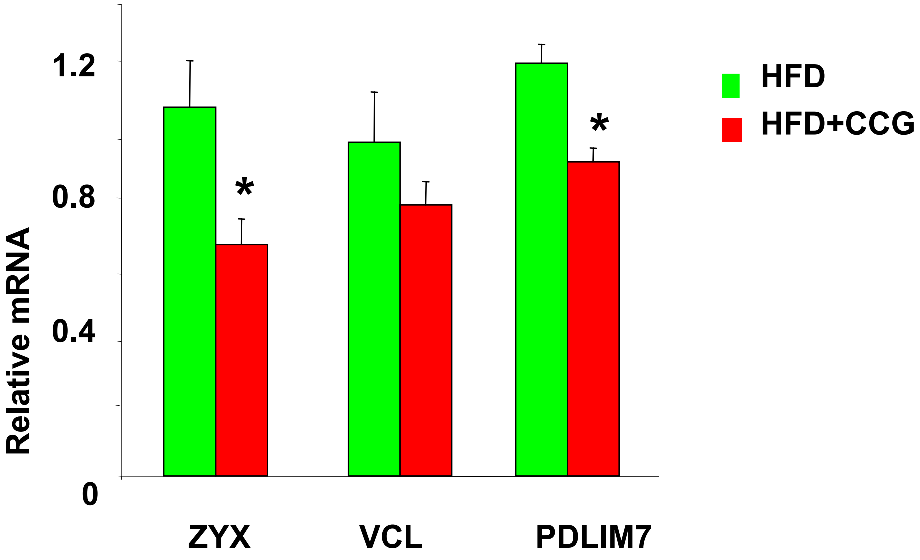

Supplemental Fig. 12. Jin et al

Supplementary Table 1. Clinical data (rectus abdominis muscle samples)

	Control	Obese (Insulin Resistant)
Age	32.3 ± 4.2	32 ± 3.3
BMI (kg/m2)	23.9 ± 2.4	49.8 ± 2.7
Hgb A1c	5.1 ±0.1	5.2 ± 0.1
Fasting glucose (mM)	4.5 ± 0.3	5.1 ± 0.1
Fasting insulin (pmol/L)	102.8 ± 5.6	206.9 ± 7.6 #
Cholesterol (mg/dL)	209 ± 25	219 ± 31 #
HDL (mg/dL)	48 ± 6	44 ± 3 #
LDL (mg/dL)	142 ± 21	157 ± 23
TG (mg/dL)	98 ± 27	135 ± 30

Supplementary Table 1. Jin et al

Supplemental Table 2. Clinical data (human myotube donors)

	Number	Age (years)	BMI (kg/m2)	Fasting Glucose (mg/dl)	Family History
Normal	8	48.0 ± 3.4	27.1 ± 1.6	94.9 ± 6.9	1/8
DM2/IR	6	59.7 ± 3.3 *	33.4 ± 3.6	109.8 ± 11.4	3/6

Supplemental Table 2. Jin et al

Supplemental Table 3. Ontology Asssessment of SRF Target Genes Altered in T2DM

GO Term	Count	%	p Value	Fold Enrichment	Bonferroni	Benjamini	FDR
GO:0044449~contractile fiber part	10	20	1.04E-10	25	0.000	0.000	0.000
GO:0043292~contractile fiber	10	20	1.94E-10	24	0.000	0.000	0.000
GO:0030016~myofibril	9	18	2.84E-09	23	0.000	0.000	0.000
GO:0003779~actin binding	12	24	9.47E-09	10	0.000	0.000	0.000
GO:0030017~sarcomere	8	16	3.26E-08	24	0.000	0.000	0.000
GO:0015629~actin cytoskeleton	10	20	2.07E-07	11	0.000	0.000	0.000
GO:0008092~cytoskeletal protein binding	12	24	8.61E-07	7	0.000	0.000	0.001
GO:0030029~actin filament-based process	9	18	1.55E-06	10	0.001	0.001	0.002
GO:0006928~cell motion	11	22	3.89E-06	7	0.003	0.002	0.006
GO:0005856~cytoskeleton	16	32	9.73E-06	4	0.001	0.000	0.012
GO:0005925~focal adhesion	6	12	2.26E-05	17	0.003	0.000	0.027
GO:0005924~cell-substrate adherens junction	6	12	2.72E-05	16	0.004	0.001	0.032
GO:0031674~I band	5	10	3.40E-05	26	0.005	0.001	0.041
GO:0030055~cell-substrate junction	6	12	3.55E-05	15	0.005	0.001	0.042

Supplemental Table 4. Primer Sequences for qRT-PCR.

HUMAN	**REVERSE PRIMER**	**FORWARD PRIMER**
CTNNA2	5'-CCCTGTATCTCCTAGGCATCAAGA-3'	5'-ACTGCACTTTGCCTCCATCAGGTA-3'
EGR2	5'-TGCCCATGTAAGTGAAGGTCTGGT-3'	5'-ACGTCGGTGACCATCTTTCCCAAT-3'
ELK1	5'-TTGGCATGGTGGAGGTAACAGACA-3'	5'AAGAACATCATCCGCAAGGTGAGC-3'
MKL1	5'-GCACAGGGCTGATTTGGTCTTGAT-3'	5'AGAGCTGAAGCAGGAGCTGAAGTT-3'
MYSM1	5'-TCAAATTAGGCTAGTAAGGTGGGA-3'	5'-GCTTATTCTCTAGATTGTCAGTACCGT-3'
NR4A1	5'-AGTCCTTGTTAGCCAGGCAGATGT-3'	5'-TCCATGCCAGCATTATGGTGTCCG-3'
PDLIM7	5'-GTTTATTCCATGCCCAAGGCAGCA-3'	5'-TTCATCTGACACTGCCTTCCCTCT-3'
SRF	5'-AGAGGTGCTAGGTGCTGTTTGGAT-3'	5'-TGAGTGCCACTGGCTTTGAAGAGA-3'
STARS	5'-TCGTAAGTCTTGCTGACCACCGTT-3'	5'-ATGGACAAAGCTCAGAGAAAGCCC-3'
TPM1	5'-TCAGCTTGTCGGAAAGGACCTTGA-3'	5'-GGCAAATGTGCCGAGCTTGAAGAA-3'
VCL	5'TAGACCACTTGGTAGCTTCCCGAT-3'	5'-GTTAATGCCATCCAATCAGCCGGT-3'
ZYX	5'-GCAGCCATTGTCATCTGCCTCAAT-3'	5'-CCCTGGACAAGAACTTCCACATGA-3'
MOUSE		
PDLIM7	5'-TCATCCGGGTCTTGCATGAACTCT-3'	5'-AGGTGCAGACCTCTGACAAACAGT-3'
STARS	5'-AGACGAGATGGCAAGATCCAGGTT-3'	5'-ATCAGCGGTGAGTGGATTTGTTGC-3'
VCL	5'-AGCATAGTGGCCTTCACTGTGGAT-3'	5'-AAGGATATCGCCAAGGCCTCTGAT-3'
ZYX	5'-TGGAAGGAGGTCCATCTCAACTCA-3'	5'-AAGTGTGAGGACTGTGGGAAACCT-3'

Supplementary Information Figure and Table Legends

Supplementary Figure 1. (A) Volunteers were recruited based on established diabetes (T2D) or diabetes family history (FH+, one or two parents with T2D), with FH- subjects (no T2D in first-degree relatives) as controls. Quadriceps muscle biopsies were performed, and RNA extracted for expression analysis using Affymetrix U133 2.0 Plus arrays. (**B**) qRT-PCR analysis of expression of additional SRF target genes in human skeletal muscle. * $p<0.05$. (**C**) SRF target protein expression in quadriceps muscle of mice fed either chow or HFD (upper panel) and quantification (lower panel).

Supplementary Figure 2. Expression of representative SRF target genes is significantly increased in muscle from muscle-specific insulin receptor knockout (MIRKO) mice. Data were obtained from Affymetrix U74Av2 expression arrays (n=8 for lox control, n=7 for MIRKO), * $p<0.05$

Supplementary Figure 3. (**A**) mRNA expression of SRF and its cofactors MKL1 and ELK1 does not differ in muscle from either FH+ or T2D, as compared with FH- subjects (n=15 FH-, 25 FH+, 11 T2D). (**B**) RhoA activity was measured in rectus abdominus muscles from control subjects undergoing elective cholecystectomy (n=4) or obese subjects undergoing gastric bypass surgery with or without T2D (n=4).

Supplementary Figure 4. Analysis of DNA-binding arrays (purchased from Panomics, Fremont, CA) hybridized as per manufacturer's protocol with nuclear extracts derived from control individuals vs. subjects with T2D (n=3 per group). Xaxis demonstrates $\log_2$ fold change of intensity (T2D/control), while y-axis demonstrates p value for between-group comparison. Note that SRF-SAP indicates oligonucleotide GTTCCGAAAGTTGCCTTTTATGG; sequence is derived from β-act in proximal SRE with flanking Ets motif sequence (Treisman,R., Marais,R., and Wynne,J. 1992. Spatial flexibility in ternary complexes between SRF and its accessory proteins. *EMBO J* 11:4631-4640). .

Supplementary Figure 5. A. MKL1 translocates to the nucleus in cells incubated with the saturated fatty acid palmitate. Graph presents results of scoring (by a blinded observer) of MKL1 localization in C2C12 myoblasts treated with either BSA or FFA (palmitate, 16:0, 250 μM, conjugated to BSA, for 16 hours). C: cytosol, N: nucleus, C=N: equal localization to cytosol and nucleus. An average of 100 cells per condition was counted. B. Palmitate activates the SRE, as demonstrated by luciferase activity using the 4X CArG construct; inset demonstrates serum-stimulated effect, for comparison.

Supplementary Figure 6. G actin staining (DNase I, Texas Red) is reduced in muscle from humans with obesity compared to lean controls undergoing elective abdominal surgery (representative photos from total of 5 subjects per group).

Supplementary Figure 7. Effects of β-actin mutants. (**A**) Overexpression of mutant β-actin in L6 myoblast. Note that R62D mutant expression was associated with reduced filamentous actin. (**B**) G15S mutant stimulates, but R62D mutant significantly suppresses SRF promoter activity.

Supplementary Figure 8. MLK1 localization and expression modulates basal and insulin-stimulated glucose uptake. L6 myoblasts expressing Myc-tagged GLUT4 were transfected with: (A) either full-length (FL) or constitutively nuclear MLK1 (SA), or (B) scrambled siRNA or siRNA targeted against MKL1. Cells were differentiated for 3 days prior to glucose uptake assay in 6 well plates. N= 5-6 per condition.

Supplementary Figure 9. Quantification of efficiency of shSTARS to reduce expression at both mRNA (A) and protein levels (B) (n=3 per group).

Supplementary Figure 10. CCG 1423 represses serum-induced SRF transcription activity (n=3 per group).

Supplementary Figure 11. CCG-1423 alters localization of MKL1 in both basal and 0.5 mM palmitate-treated cells. CCG-1423 reverses MKL1 nuclear accumulation. C: cytosol, N: nucleus; C=N: equal localization to cytosol and nucleus. An average of 115 cells were counted per condition.

Supplementary Figure 12. Expression of SRF target genes (e.g. ZYX, VCL, PDLIM7) in quadriceps muscle significantly decreases after CCG-1423 administration. N=7 per group.

Supplementary Table 1. Demographic data for human subjects from whom rectus abdominus samples were obtained for G-actin staining demonstrated in Supplementary Figure 5. n=5 per group.

Supplementary Table 2. Demographic data for subjects from whom primary myotubes were isolated (n=8 for controls, 6 for IGT/DM).

Supplementary Table 3. Gene ontology analysis of 54 SRF-regulated genes (Figure 1A). Analysis was performed using DAVID (http://david.abcc.ncifcrf.gov/).

Supplementary Table 4. Primer sequences used for qRT-PCR.